

# ESI for “Bayesian determination of the effect of a deep eutectic solvent on the structure of lipid monolayers”

Andrew R. McCluskey,<sup>ab‡</sup> Adrian Sanchez-Fernandez,<sup>ac‡¶</sup>  
Karen J. Edler,<sup>a\*</sup> Stephen C. Parker,<sup>a</sup> Andrew J. Jackson,<sup>cd</sup>  
Richard A. Campbell,<sup>ef</sup> and Thomas Arnold<sup>abcg\*</sup>

<sup>a</sup> Department of Chemistry, University of Bath, Claverton Down, Bath, BA2 7AY, UK.

<sup>b</sup> Diamond Light Source, Harwell Campus, Didcot, OX11 0DE, UK.

<sup>c</sup> European Spallation Source, SE-211 00 Lund, Sweden.

<sup>d</sup> Department of Physical Chemistry, Lund University, SE-211 00 Lund, Sweden.

<sup>e</sup> Institut Laue-Langevin, 71 avenue des Martyrs, 38000, Grenoble, France.

<sup>f</sup> Division of Pharmacy and Optometry, University of Manchester, Manchester, M13 9PT, UK.

<sup>g</sup> ISIS Neutron and Muon Source, Science and Technology Facilities Council, Rutherford Appleton Laboratory, Harwell Oxford, Didcot OX11 0QX, UK.

¶ Present address: Department of Food Technology, Lund University, SE-211 00 Lund, Sweden

## 1 Grazing incident X-ray diffraction (GIXD)

GIXD was measured for DPPC and DMPC at  $30\text{ mN m}^{-1}$  at  $22^\circ\text{C}$  (and  $7^\circ\text{C}$  for DMPC), and are shown in Figures 1-3. All figures contain an artifact from the X-ray beam interacting with the Teflon of the Langmuir trough. However, in figures 1 and 3 it is possible to identify a (2, 0) diffraction peak that indicates the presence of a similar structure to that found under the same conditions in water.<sup>1</sup> Based on this information we believe that, similar to water, the phase of the lipid tails is likely to be in the liquid phase at all surface pressures measured.

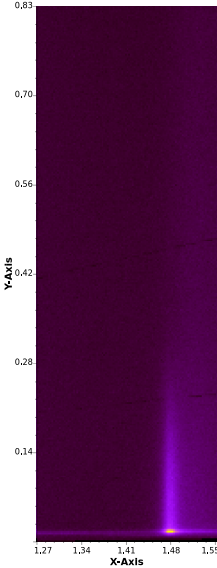


Figure 1: The GIXD pattern for DPPC at  $30 \text{ mN m}^{-1}$  at  $22^\circ\text{C}$ , the axes at in units of  $\text{\AA}^{-1}$ . Source: Datasets, figure files and running/plotting scripts are available under CC-BY.<sup>2</sup>

## 2 Probability distribution functions

The two-dimensional probability distribution functions (PDFs) for all parameters and all lipids from the X-ray reflectometry models are given in Figures 4-19. The two-dimensional probability distribution functions (PDFs) for all parameters and all lipids from the neutron reflectometry models are given in Figures 20-23.

## References

- [1] E. B. Watkins, C. E. Miller, D. J. Mulder, T. L. Kuhl, and J. Majewski, *Phys. Rev. Lett.*, 2009, **102**, 238101.
- [2] A. McCluskey, *Figures for "Bayesian determination of the effect of a deep eutectic solvent on the structure of lipid monolayers"*, 2018, [https://figshare.com/articles/\\_/6661784/0](https://figshare.com/articles/_/6661784/0).

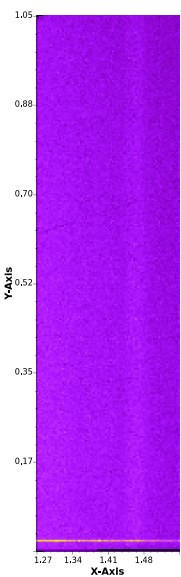


Figure 2: The GIXD pattern for DMPC at  $30 \text{ mN m}^{-1}$  at  $22^\circ\text{C}$ , the axes at in units of  $\text{\AA}^{-1}$ . Source: Datasets, figure files and running/plotting scripts are available under CC-BY.<sup>2</sup>

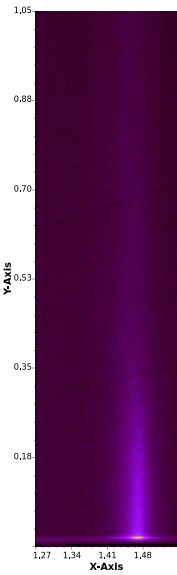


Figure 3: The GIXD pattern for DMPC at  $30 \text{ mN m}^{-1}$  at  $7^\circ\text{C}$ , the axes at in units of  $\text{\AA}^{-1}$ . Source: Datasets, figure files and running/plotting scripts are available under CC-BY.<sup>2</sup>

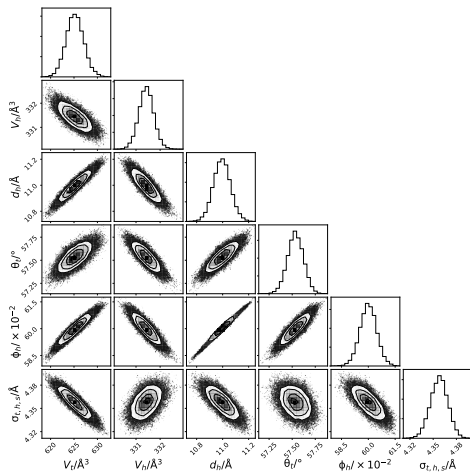


Figure 4: The multi-parameter PDFs for the chemically-relevant model of DLPC X-ray reflectometry data at  $20 \text{ mNm}^{-1}$ . Source: Datasets, figure files and running/plotting scripts are available under CC-BY.<sup>2</sup>

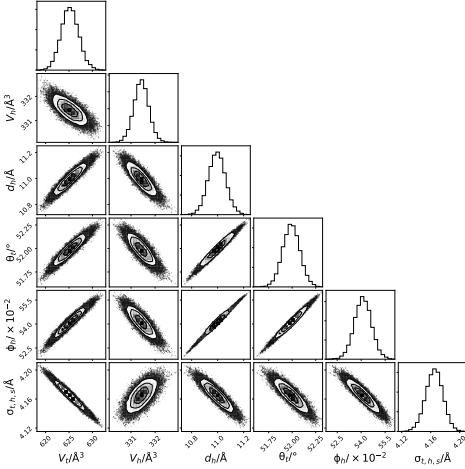


Figure 5: The multi-parameter PDFs for the chemically-relevant model of DLPC X-ray reflectometry data at  $25 \text{ mNm}^{-1}$ . Source: Datasets, figure files and running/plotting scripts are available under CC-BY.<sup>2</sup>

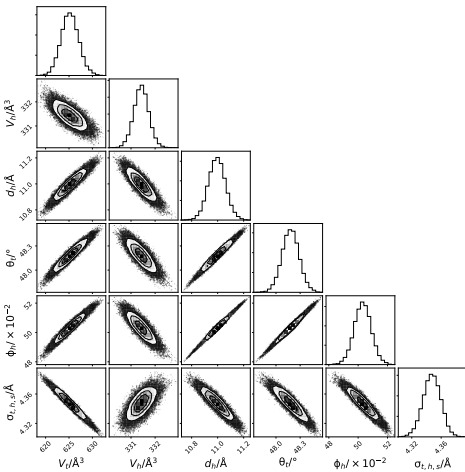


Figure 6: The multi-parameter PDFs for the chemically-relevant model of DLPC X-ray reflectometry data at  $30 \text{ mNm}^{-1}$ . Source: Datasets, figure files and running/plotting scripts are available under CC-BY.<sup>2</sup>

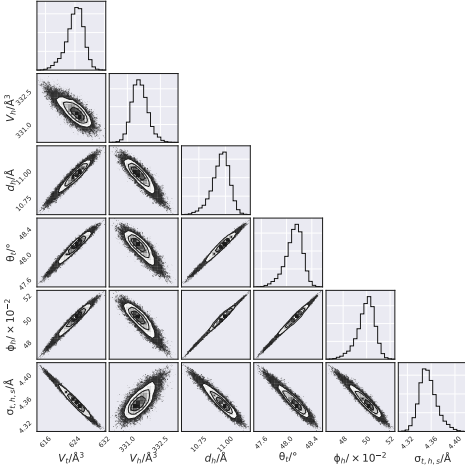


Figure 7: The multi-parameter PDFs for the chemically-relevant model of DLPC X-ray reflectometry data at 35 mNm<sup>-1</sup>. Source: Datasets, figure files and running/plotting scripts are available under CC-BY.<sup>2</sup>

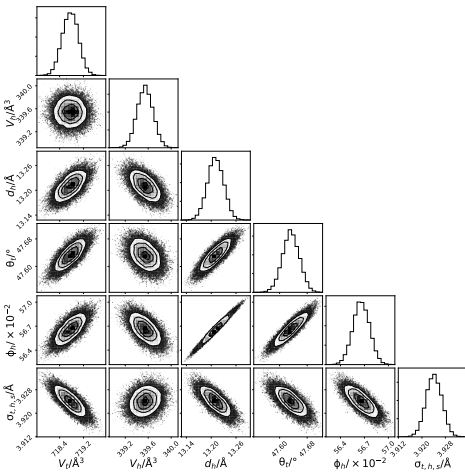


Figure 8: The multi-parameter PDFs for the chemically-relevant model of DMPC X-ray reflectometry data at 20 mNm<sup>-1</sup>. Source: Datasets, figure files and running/plotting scripts are available under CC-BY.<sup>2</sup>

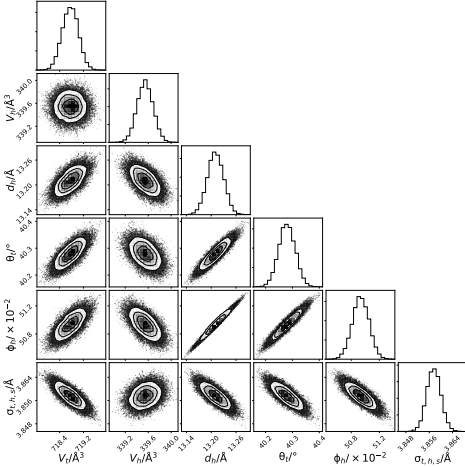


Figure 9: The multi-parameter PDFs for the chemically-relevant model of DMPC X-ray reflectometry data at  $25 \text{ mNm}^{-1}$ . Source: Datasets, figure files and running/plotting scripts are available under CC-BY.<sup>2</sup>

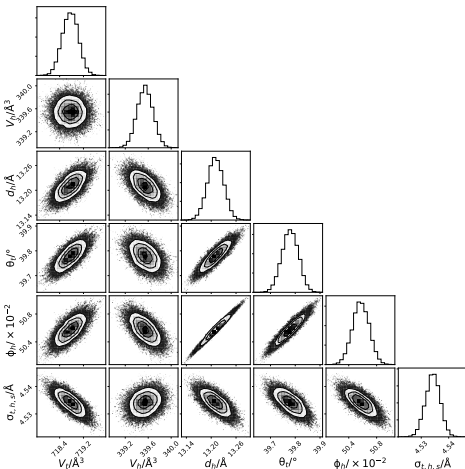


Figure 10: The multi-parameter PDFs for the chemically-relevant model of DMPC X-ray reflectometry data at  $30 \text{ mNm}^{-1}$ . Source: Datasets, figure files and running/plotting scripts are available under CC-BY.<sup>2</sup>

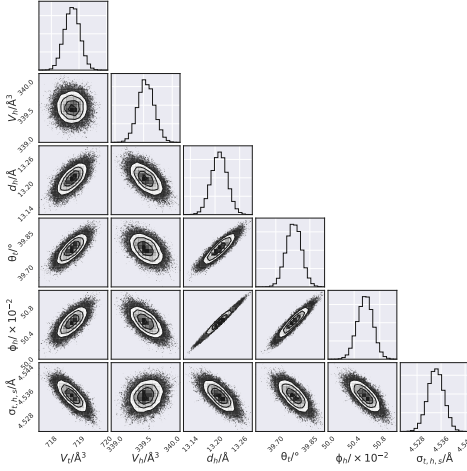


Figure 11: The multi-parameter PDFs for the chemically-relevant model of DMPC X-ray reflectometry data at  $40 \text{ mNm}^{-1}$ . Source: Datasets, figure files and running/plotting scripts are available under CC-BY.<sup>2</sup>

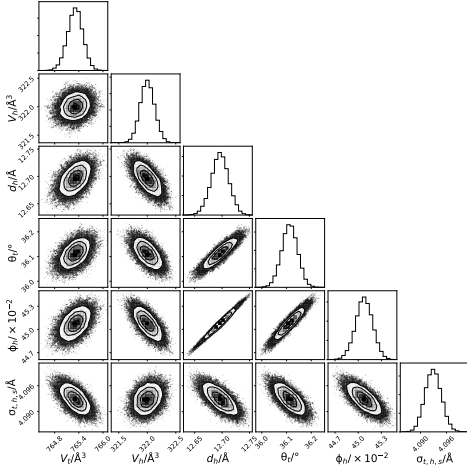


Figure 12: The multi-parameter PDFs for the chemically-relevant model of DPPC X-ray reflectometry data at  $15 \text{ mNm}^{-1}$ . Source: Datasets, figure files and running/plotting scripts are available under CC-BY.<sup>2</sup>

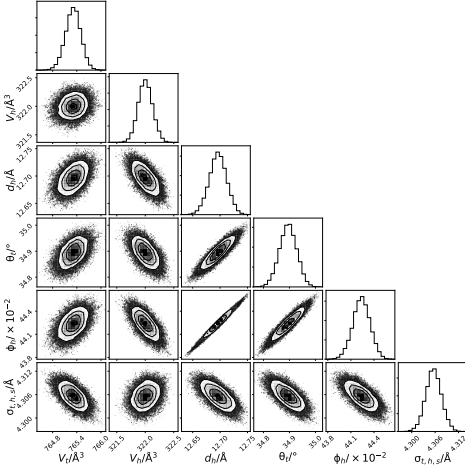


Figure 13: The multi-parameter PDFs for the chemically-relevant model of DPPC X-ray reflectometry data at  $20 \text{ mNm}^{-1}$ . Source: Datasets, figure files and running/plotting scripts are available under CC-BY.<sup>2</sup>

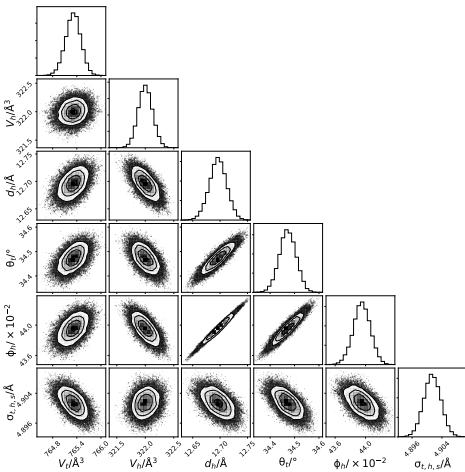


Figure 14: The multi-parameter PDFs for the chemically-relevant model of DPPC X-ray reflectometry data at  $25 \text{ mNm}^{-1}$ . Source: Datasets, figure files and running/plotting scripts are available under CC-BY.<sup>2</sup>

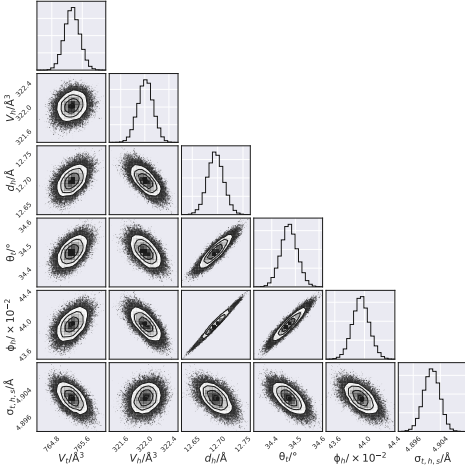


Figure 15: The multi-parameter PDFs for the chemically-relevant model of DPPC X-ray reflectometry data at  $30 \text{ mNm}^{-1}$ . Source: Datasets, figure files and running/plotting scripts are available under CC-BY.<sup>2</sup>

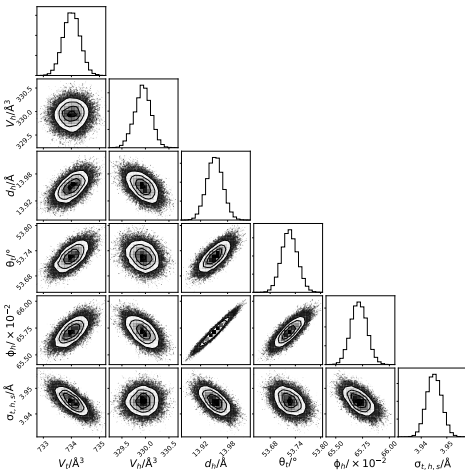


Figure 16: The multi-parameter PDFs for the chemically-relevant model of DMPG X-ray reflectometry data at  $15 \text{ mNm}^{-1}$ . Source: Datasets, figure files and running/plotting scripts are available under CC-BY.<sup>2</sup>

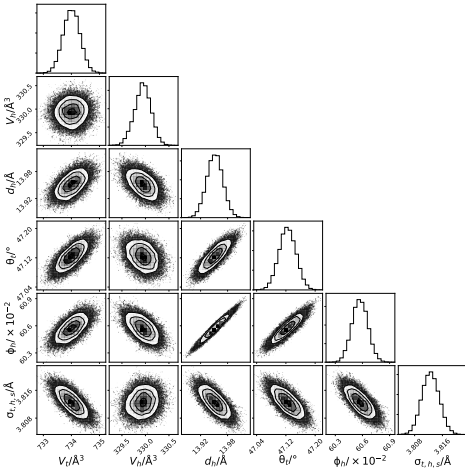


Figure 17: The multi-parameter PDFs for the chemically-relevant model of DMPG X-ray reflectometry data at  $20 \text{ mNm}^{-1}$ . Source: Datasets, figure files and running/plotting scripts are available under CC-BY.<sup>2</sup>

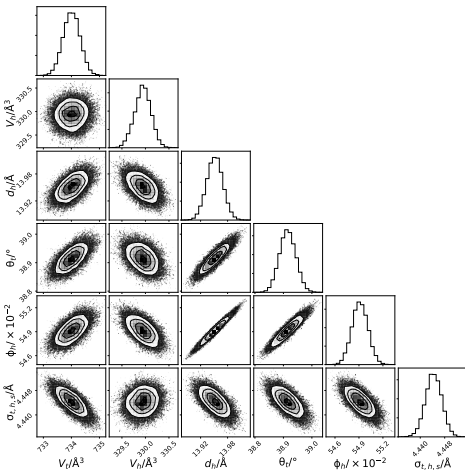


Figure 18: The multi-parameter PDFs for the chemically-relevant model of DMPG X-ray reflectometry data at  $25 \text{ mNm}^{-1}$ . Source: Datasets, figure files and running/plotting scripts are available under CC-BY.<sup>2</sup>

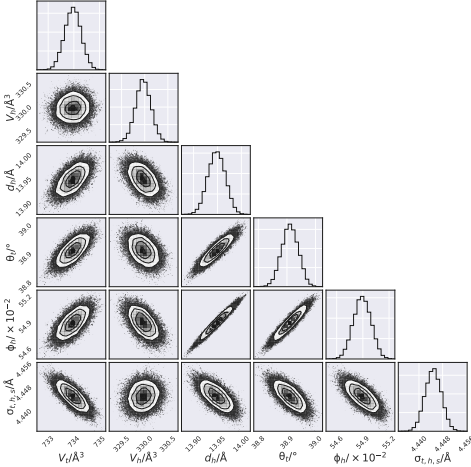


Figure 19: The multi-parameter PDFs for the chemically-relevant model of DMPG X-ray reflectometry data at  $30 \text{ mNm}^{-1}$ . Source: Datasets, figure files and running/plotting scripts are available under CC-BY.<sup>2</sup>

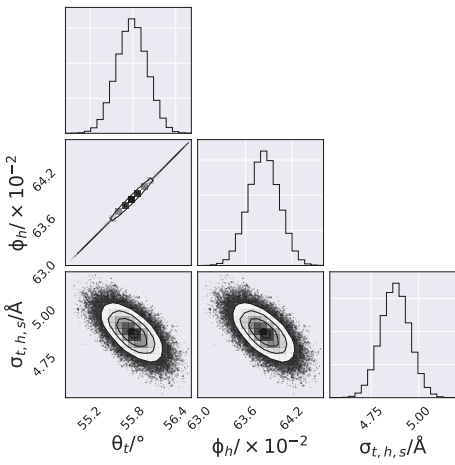


Figure 20: The multi-parameter PDFs for the chemically-relevant model of two contrast DMPC neutron reflectometry data at  $20 \text{ mNm}^{-1}$ . Source: Datasets, figure files and running/plotting scripts are available under CC-BY.<sup>2</sup>

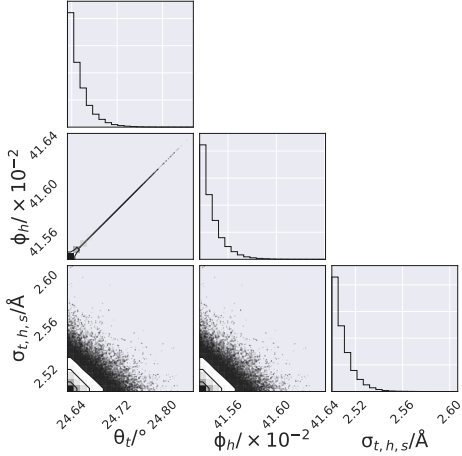


Figure 21: The multi-parameter PDFs for the chemically-relevant model of two contrast DMPC neutron reflectometry data at  $25 \text{ mNm}^{-1}$ . Source: Datasets, figure files and running/plotting scripts are available under CC-BY.<sup>2</sup>

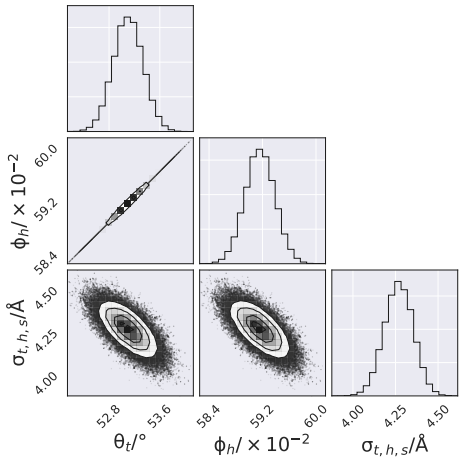


Figure 22: The multi-parameter PDFs for the chemically-relevant model of two contrast DPPC neutron reflectometry data at  $15 \text{ mNm}^{-1}$ . Source: Datasets, figure files and running/plotting scripts are available under CC-BY.<sup>2</sup>

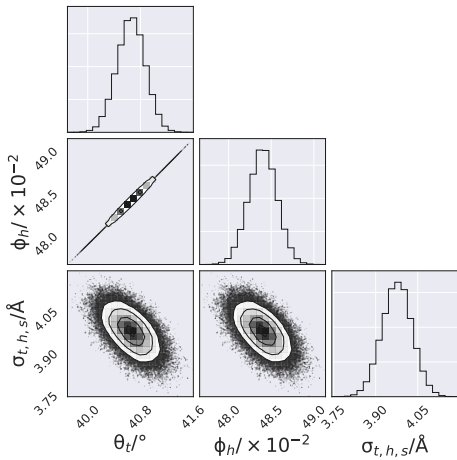


Figure 23: The multi-parameter PDFs for the chemically-relevant model of two contrast DMPC neutron reflectometry data at  $20 \text{ mNm}^{-1}$ . Source: Datasets, figure files and running/plotting scripts are available under CC-BY.<sup>2</sup>